BEHAVIOUR OF ALUMINA REFRACTORY COMPOSITES FOR TEMPERATURES BELOW 800°C. EXPERIMENT AND MODELLING

J.F. Hernandez [1, 3], N. Schmitt [1], P. Meunier[2], and J. Poirier [3]

[1] *LMT-Cachan (ENS de Cachan, CNRS, Université Paris 6)*
61, avenue du Président Wilson, F-94 235 Cachan Cedex, France
[2] *Lafarge Monolitiques Réfractaires*
97, avenue Aristide Briand, F-92 120 Montrouge, France
[3] *CRDM / SOLLAC,*
Grande Synthe, BP 2508, F-59 381 Dunkerque, France

SUMMARY: A study of the changes in the chemical, physical and mechanical properties of high alumina refractory castables was made for temperature below 800°C. The aim was to estimate the effects of the conversion of the hydrates contained in the binder. First, the principal steps of the dehydration were determined by X-Ray Diffraction and thermal analysis. Constitutive equations were proposed to characterise the phase transformations of the binder. The material parameters were identified by thermogravimetric analysis. Then, both the porosity of the cement paste, measured by mercury intrusion porosimetry, and the thermal shrinkage, measured by thermal dilatation tests were modelled using the previous chemical identification. Finally, the influence of the dehydration on the global properties of composites containing alumina-based aggregates was studied. Experimental data of the thermal shrinkage and Young's modulus obtained on composites with different aggregates contents were compared with a micromechanical model.

KEYWORDS: concrete, alumina, dehydration, thermal analysis, modelling

INTRODUCTION

Alumina refractories are used in a severe thermal environment because of their good resistance at high temperatures. In particular, they are used in steelmaking for both steel laddle linings and precast pieces such as burners. Moreover, complex geometry of structures can be easily shaped. In the past, many studies have been made to increase the performances of the chemical, physical and mechanical properties in both fresh and hardened states, notably by changing of the distribution of aggregates sizes, adding fused alumina and silica fume particles and admixtures. Thanks to these improvements, it was possible to reduce both the cement and water contents and thus to gain in mechanical resistance, wear resistance and corrosion at high temperatures. Today, the manufacturer proposes a wide range of products with physical and chemical properties for various uses.

The high temperature properties of castable were widely studied in the past, while less attention was given to lower temperature properties. Nevertheless, the latter are of great

importance because the states of stresses and strains in structures depend on the history of the temperature loading.

In this paper, we will examine the connection between some chemical and physico-mechanical properties of refractories depending on the composition of the castable. This work is the first part to the global comprehension of the coupling between phases transformation and physical mechanical properties of castable at temperatures in use. It was limited to the dehydration process that occurs at temperatures below 800°C.

INITIAL COMPOSITION OF ALUMINA CONCRETE

The compounds of two typical castables were used as basic compounds for the analysis. One had a high cement content (HCC) and the other one had an ultra low cement content (ULCC) (Table 1). The castables were composed of high alumina aggregates and a hydrated alumina cement paste. The aggregates were composed of coarse bauxite grains with sizes between 0.1 mm and 5 mm and fine calcined alumina particles (1-10 μm). These grains did not react in the temperature range 0 to 1000°C. In the ULCC, 4 % in weight of silica fume particles (0,3 μm) were added.

Castable	Weight of cement (%)	Weight of aggregates (%)	Water / cement
HCC	20	65	0.5
ULCC	2	65	2.7

Table 1: composition in weight and volume of castables

The cement was SECAR 71 marketed by Lafarge Aluminate containing essentially monocalcium aluminate CA (61 % in weight) and bi-calcium aluminate CA_2 (37.5 % in weight) [1]. For convenience the cement chemist abbreviations are used in the text: C = CaO, $A=Al_2O_3$, $H=H_20$. The hydration process of these anhydres was widely studied in the past. The chemical composition of the hydrates was shown to depend on curing temperature. At room temperature (below 25 °C) a thermodynamically unstable CAH_{10} hydrate is formed which tends to convert progressively into more stable hydrates. At slightly higher temperature (below 35 °C), an unstable C_2AH_8 hydrate is formed. For higher temperatures, these hydrates turn into two stable hydrates AH_3 and C_3AH_6.

In the refractory world, the reference state of the cement based material is usually the state obtained after heat treatment to eliminate the non chemically combined water and to obtain the stable hydrates of specimens. In this study, all specimens (cement paste and composites) were dried at 110 °C for 48 hours.

DEHYDRATION PROCESS OF THE CEMENT PASTE

Experimental results

Secar 71 cement was mixed with water in mass proportion ratio water to cement (w/c) of 0.3. From the stoechiometric analysis and estimation of the free water content, it resulted that at the reference's state only 70 % in weight of the compounds were hydrates.

The dehydration process of a hydrated cement paste (not cured at 110°C) was investigated by thermogravimetric analysis (TGA) (see Fig. 1) and thermal differential analysis (TDA). Complementary investigation by X-Ray diffraction (XRD) analysis was made on specimen heated at different temperatures (up to 600°C). The following conclusions were obtained.

Up to a temperature of about 110 °C, the hydration process continue until completed. The mass loss was due to the progressive elimination of both the free water (nearly 5 % of initial water content) and the water which was released by the conversion of unstable hydrates **into** stable hydrates AH_3 and C_3AH_6 and which was not used to form new hydrates. For higher temperatures, up to 600°C the mass loss was due to both progressive decomposition of the hydrates and elimination of the chemically combined water. The different peaks of mass loss rate showed that several reactions were activated at different temperatures. XRD analysis on specimens heat-treated at 600°C had shown that the hydrates had disappeared. For higher temperatures, mineralogically structural changes of the compound were observed by DTA and XRD analysis but had not led to a mass loss.

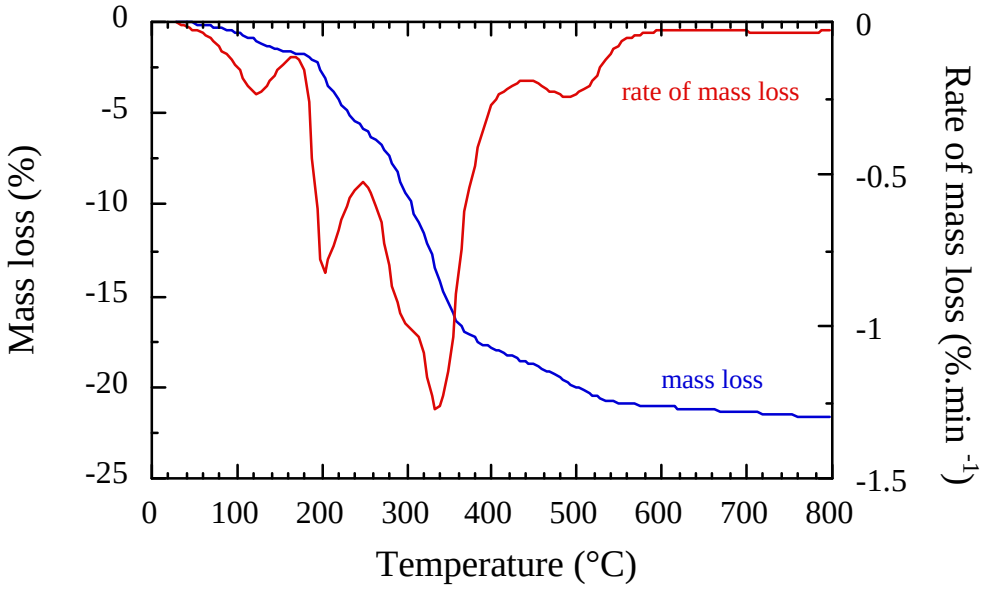

Figure 1: TGA-analysis of hydrated SECAR 71 cement (temperature increase rate of 10 °C.min^{-1})

TGA made with different temperature loading paths had shown a strong dependence to the heating rate. As an example the mass loss of a specimen heated up to 210 °C and held at this temperature for several hours was about 15 % instead of 4 % when the specimen was heated up to 210 °C at 10 °C.min^{-1}.

Modelling of the kinetic of the dehydration process

In a first approximation the decomposition of each hydrate is carried out in two steps and may be described by the following stoechiometric reactions [1] [2] [3].

$$AH_3 \rightarrow AH + 2H \quad (1)$$

$$AH \rightarrow A + H \quad (2)$$

$$C_3AH_6 \rightarrow C_3AH_{1.5} + 4.5H \quad (3)$$

$$C_3AH_{1.5} \rightarrow (C_{12}A_7, CA, A, ...) + 1.5H \quad (4)$$

The following simplification of the dehydration process, viewed in the case of gibbsite in figure 2, is proposed. The hydrates are supposed to be grouped into spheres of identical initial radius. When the temperature T exceeds T_1, the first spherical shell of reacting phase AH occurs and grows radially towards the centre of the composite sphere. Reaction takes place on the interface of the two hydrates and the water vapour diffused through the shell. When the temperature T exceeds T_2, a new spherical shell of alumina phase occurs due to the second reaction and progress radially too.

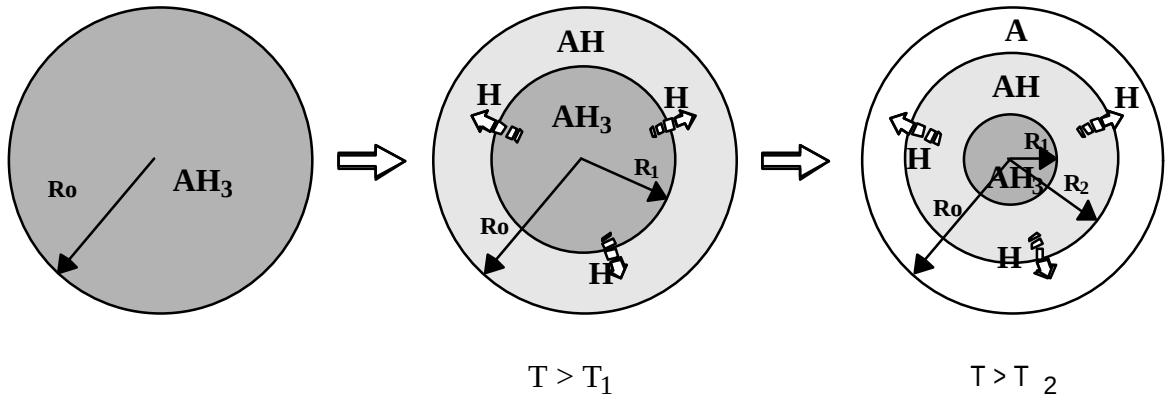

Figure 2: topology of the decomposition process of AH_3

If ζ_i is the degree of conversion of hydrate ($0 < \zeta_i < 1$) the evolution laws of the first step of decomposition can be written as

$$\begin{aligned} T \geq T_i \quad \text{then} \quad & \frac{d\zeta_i}{dt} = -K_i(1-\zeta_i)^n.T^m \exp(-\frac{E_i}{RT}) \\ T < T_i \quad \text{then} \quad & \frac{d\zeta_i}{dt} = 0 \qquad i = \{1,3\} \end{aligned} \quad (5)$$

The evolution laws of the second step of the dehydration are given by:

$$T < T_i \quad \text{then} \quad \frac{d\zeta_i}{dt} = 0 \qquad i = \{2,4\}$$

$T \geq T_i$ then

$$* \ \zeta_i < \zeta_{i-1} \quad \text{then} \quad \frac{d\zeta_i}{dt} = -K_i (1-\zeta_i)^n . T^m \exp\left(-\frac{E_i}{RT}\right) \tag{6}$$

$$* \ \zeta_i = \zeta_{i-1} \quad \text{then} \quad \frac{d\zeta_i}{dt} = \frac{d\zeta_{i-1}}{dt}$$

In these expressions, E_i are the activation energy, K_i the kinetic parameter, n the exponent of the reaction. Considering here three-dimensional phase boundary reactions and no flow resistance of the water vapour through the porous shells it results that n is equal to 2/3. The parameter m is an exponent which can have different values for example in accordance with the collision theory (m=0.5) or transient theory (m=1) [4]. m = 0 is used in this study so that the temperature influence correspond to the classical Arrhenius relation.

The results of seven TGA with different temperature loading paths and the chemical composition of the hydrates were used to identify the parameters of the kinetic model. It appeared that the use of a multi-step reactions analysis had permitted to fit the different experimental curves accurately (figure 3). As the parameters are independent of the hydrates content, it is possible to predict with the same set of parameters the mass loss of cement paste with other initial w/c ratio.

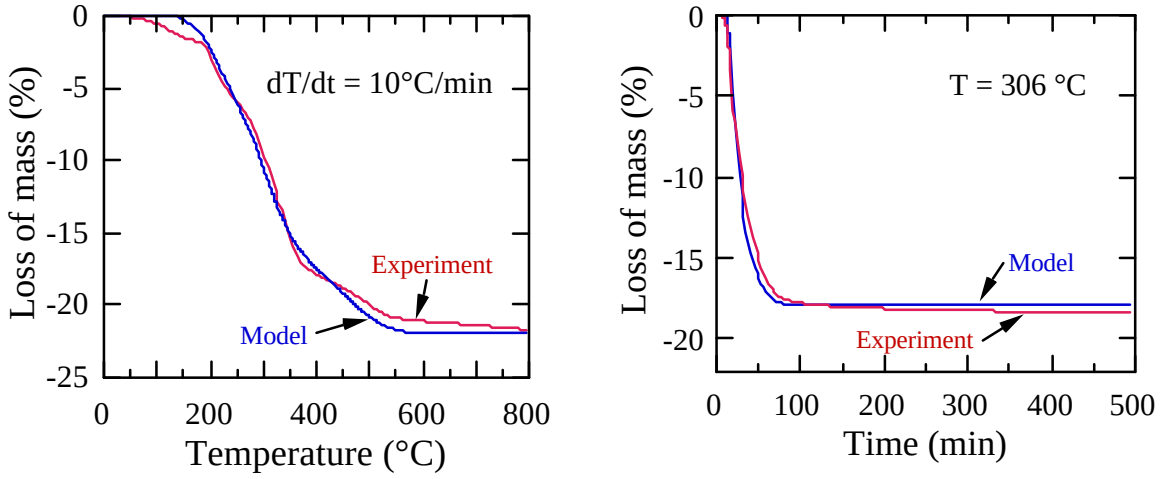

a) constant temperature rate loading

b) fast temperature loading followed by a up holding at 306 °C

Figure 3: Identification of the parameters of the kinetic reaction model

POROSITY AND SHRINKAGE OF THE CEMENT PASTE

The specimens were treated at different temperatures and the open porosity was measured by mercury intrusion porosimetry test. The results showed that the porosity had increased from 14 % to 24 % (fig. 4a). The thermal dilatation of cylinders (25 mm diameter and 50 mm length) was also measured by differential displacement measurement. When the specimen was heated for the first time, an irreversible contraction appeared in the 150°C-450°C temperature range (fig. 4b). It corresponded to a volumetric contraction of about 4 % and did not appear when the specimen was heated again after cooling.

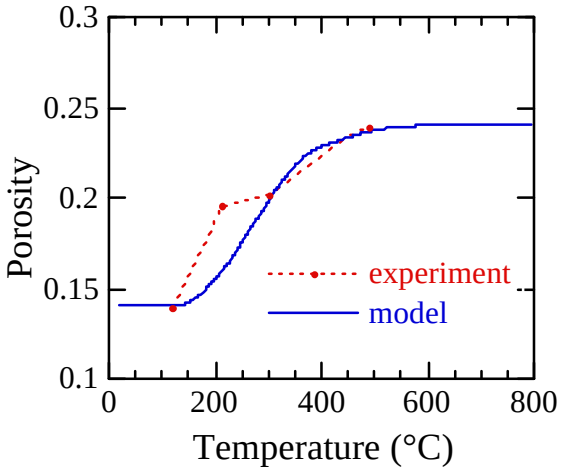

a) porosity vs temperature of treatment of the specimen

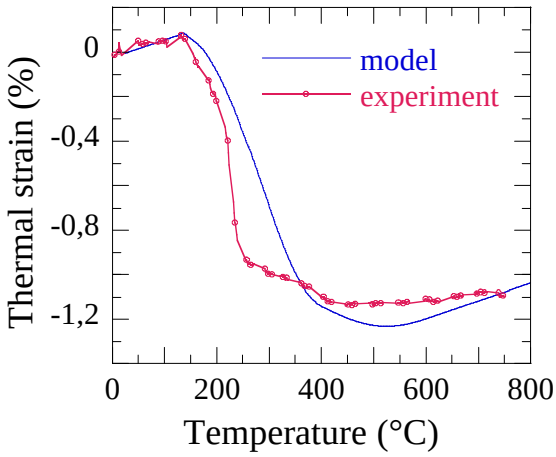

b) evolution of thermal dilatation strain vs temperature during the first heating

Figure 4: comparison between experiments and modelling for the cement paste

The high reduction in the volume of hydrates during the conversion was the cause of the shrinkage. However, because of incompatibilities of the strains in the different phases of the paste, the porosity increased and the shrinkage was lower than expected.

The chemical volumetric shrinkage (stress-free hypothesis) of hydrates AH_3 and C_3AH_6 ($\varepsilon_{vA}^{thsh}(\zeta_1,\zeta_2)$ and $\varepsilon_{vC}^{thsh}(\zeta_3,\zeta_4)$) are computed considering the theoretical densities and their degree of dehydration. Then, the increase in the porosity is calculated supposing a linear variation with the chemical stress free contraction:

$$\phi(t)=\phi_o+(\phi_f-\phi_o)\frac{\varepsilon_v^{thsh}(\zeta_i(t))}{\varepsilon_v^{thsh}(\zeta_i=1)} \quad \text{with} \quad \varepsilon_v^{thsh}(\zeta_i)=\varepsilon_{vA}^{thsh}(\zeta_1,\zeta_2)+\varepsilon_{vC}^{thsh}(\zeta_3,\zeta_4) \tag{7}$$

The thermal strain is decomposed as following:

$$\varepsilon_v^{th}(\zeta_i,T)=\varepsilon_v^{\alpha}(\zeta_i,T)+\varepsilon_v^{sh}(\zeta_i) \quad \text{with} \tag{8}$$

$$\varepsilon_v^{\alpha}(\zeta_i,T)=\alpha^{hyd}(T)\left(1-\frac{\Delta m(\zeta_i)}{\Delta m(\zeta_i=1)}\right)+\alpha^{dehyd}(T)\frac{\Delta m(\zeta_i)}{\Delta m(\zeta_i=1)} \tag{9}$$

$$\varepsilon_v^{sh}(\zeta_i)=-\frac{1-\phi_o}{1-\phi(\zeta_i)}H(\varepsilon_{vA}^{thsh}(\zeta_1,\zeta_2)f_{vi}(AH_3)+\varepsilon_{vA}^{thsh}(\zeta_3,\zeta_4)f_{vi}(C_3AH_6) \tag{10}$$

In these expressions α is the thermal dilatation coefficient, f_{vi} the initial volume content of hydrates, Δm the mass loss and H an interaction parameter which takes into account for the effect of interaction between the different phases (unhydrates and hydrates). It is the only parameter to identify. A good fit of this modelling with the experimental data has been obtained (fig. 4).

PREDICTION OF THE SHRINKAGE OF THE COMPOSITE

The thermal shrinkage of industrial castable depends on the aggregates content. For the high cement content castable, an irreversible strain of about 0.23 % was reached, while for the ultra low cement castable, it was limited to 0.08 **%**. Therefore, in order to study the influence of this factor, cylinders of composites with different contents of aggregates were tested. Both the Young's modulus measured by ultra sonic device and thermal shrinkage were determined. To limit the size effect, the upper grade of the aggregates was 3.5 mm instead of 5 mm for the industrial product. Composition with a low proportion of cement also contained silica fume.
The experimental results of these two properties are reported in figures 5a and 5b. The data of the Young's modulus correspond to specimen heated at different temperatures for 48 hours.

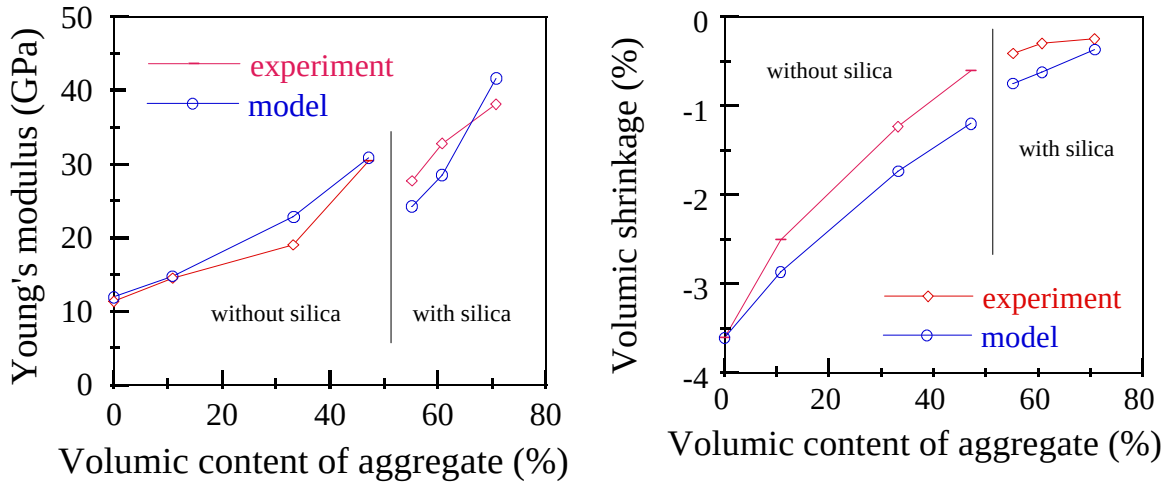

a) Young'modulus vs aggregate content for heat treated specimen

b) Shrinkage vs aggregate content

Figure 5: comparison between experiments and modelling for the castable

The shrinkage of the castable can be related to the shrinkage of the cement paste by micromechanical analysis. Recently De Larrard and Le Roy have proposed to modify the composite sphere assemblage of Hashin to take into account for the maximal aggregates proportion [5] [6]. This model has been successfully used for high strength concrete. The topology is presented in figure 6.

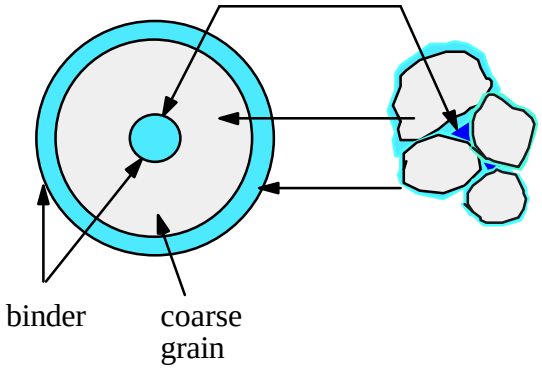

Figure 6: topology of the micromechanical model of De Larrard and Le Roy

The coarse grains are coated with only a part of the matrix phase. The other part is trapped in the void between the composite, because the most dense aggregates packing does not permit to fill up the void space (the maximal compacity is about 0.8). The following expressions for the Young's modulus and the shrinkage are obtained, supposing that the Poisson's coefficient of both phases is equal to 0.2:

$$E_r = \left[1 + \frac{2b(1-E^2)}{1-b+2(\frac{2}{a^*}-1)E+(1+b)E^2}\right] E_c \qquad (11)$$

$$\varepsilon_{vr}^{sh} = \left[\frac{(1+E)(1-b)+\frac{4E(1-a^*)b}{a^*+E(2-a^*)}}{1+b+E(1-b)}\right] \varepsilon_{vc}^{sh} \qquad (12)$$

where
E =Ec/Ea and b = a/a*,
Ec and Ea are the Young's Modulus of cementitous matrix and aggregates,
a and a* are the volumetric proportion of aggregates and the maximal volumetric proportion possible.

Figure 5 shows that the model is able to predict the experimental data with enough accuracy. The change of slope in figure 5a is due to the fact that for high content of aggregates, fine alumina and silica fume particles have been added. For this case, the micromechanical model has been applied twice. In a first step, Young's modulus and the shrinkage of a phase containing the cement paste and only the very small particles are calculated. In the second step, this phase is considered as the matrix of the castable containing coarse aggregates, so that the model is applied again.

CONCLUSION

The connection between phases transformations of the hydrated matrix and the overall physical and mechanical properties were examined. Schematic reactions of dehydration and kinetic constitutive equations were identified for a castable that did not contain silica fume. This modelisation allowed us to known the state of conversion of hydrates at any time. It was introduced in other models to explain the evolution of porosity and thermal shrinkage of the cementitous binder and later the overall stiffness and shrinkage of composite containing both hydrated matrix and inert aggregates. The model could help for modelling the thermo-mechanical model of alumina castable. In particular, it allowed us to understand the part played of the different compounds in the overall properties of castable.

REFERENCES

1. S. Plibrico, “Technology of Refractory Materials”, Japan, 1984.

2. G. Platret, “Processus de formation et propriétés des produits de déshydratation de CAH_{10}”, *PhD thesis*, Fac. des Sci. M.I.P.C. Univ. de Dijon, 1983.

3. H.J. Kuzel, “Uber die orientierte Entwässerung von Tricalciumaluminathydrat C_3AH_6”, *Neues Jahrbuch für Mineralogie Monatheft,* 397-403, 1969.

4. Brown M.E., Dollimore D. and Gallway A.K.,”Comprehensive Chemical Kinetics”, Vol. 22, Reactions in solid state, Ed. C. H. Bamford and C.F. Tipper, Amsterdam, 1980, p 57

5. De Larrard F. and Le Roy R., “The influence of mix composition on mechanical properties of high-performance silica fume concrete”, *Proceedings of the 4th Int. Conf. on Fly Ash, Silica fume, Slag and natural Pozzolans in Concrete*, Ed. by Istanbul, Turkey, Pub., may 1992.

6. Le Roy R., “Déformations instantanées et différées des bétons à hautes performances”, *PhD. thesis*, E.N.P.C. Paris, 1995.